symposium on hepatitis C virus & related viruses., San Antonio, USA, 2008.

9) Shoji, I., Osaki, M., Murakami, K., Suzuki, T., Miyamura, T., Wakita, T., and Hotta, H. Ubiquitylation signal of hepatitis C virus core protein. 15th International symposium on hepatitis C virus & related viruses., San Antonio, USA, 2008.

10) 原弘道、相崎英樹、松田麻未、村上恭子、勝二郁夫、松浦善治、宮村達男、脇田隆字、鈴木哲朗、creatine kinase B はC型肝炎ウイルス NS4A との相互作用によりウイルスゲノム複製複合体へ運ばれエネルギー供給に働く、第56回日本ウイルス学会学術集会、岡山、2008.

11) 村上恭子、阿部克俊、高宮智史、木村敬郎、鈴木哲朗、宮村達男、小池和彦、脇田隆字、勝二郁夫、HCV コア蛋白に結合する新規宿主因子 hnRNPH1/H2 の HCV 生活環における役割、第56回日本ウイルス学会学術集会、岡山、2008.

12) Lin Deng、足達哲也、北山喜久美、分玉泰彰、北澤荘平、石戸聡、勝二郁夫、堀田博、C型肝炎ウイルス感染によるアポトーシスの分子機序の解析、第56回日本ウイルス学会学術集会、岡山、2008.

13) 堀田博、北山喜久美、矢吹玲子、Lin Deng、長野基子、勝二郁夫、C型肝炎ウイルスの持続感染は宿主細胞の核小体肥大、アポトーシス感受性低下及び細胞周期進行を誘導する、第56回日本ウイルス学会学術集会、岡山、2008.

14) 浜本いつき、村上恭子、鈴木哲朗、多屋馨子、岡部信彦、脇田隆字、勝二郁夫、C型肝炎ウイルス複製を制御する宿主因子 ERGIC-53 の機能、第56回日本ウイルス学会学術集会、岡山、2008.

15) エルシャーミーアメード、足達哲也、犬伏祥子、勝二郁夫、堀田博、ペグインターフェロン/リバビリン併用療法における HCV core および NS5A の多様性による SVR 予測因子と Non-SVR 予測因子の検討、第56回日本ウイルス学会学術集会、岡山、2008.

16) 内海孝子、ルシダマリア、長野基子、笹山美紀子、勝二郁夫、堀田博、インドネシア・パプア州の B 型肝炎ウイルス(HBV)の分子系統樹解析と新規 subgenotype の同定、第56回日本ウイルス学会学術集会、岡山、2008.

17) 勝二郁夫、大崎一直、村上恭子、鈴木哲朗、宮村達男、脇田隆字、堀田博、C型肝炎ウイルスコア蛋白質のユビキチン化シグナル、第31回日本分子生物学会年会、神戸、2008.

18) 村上恭子、阿部克俊、高宮智史、木村敬郎、鈴木哲朗、宮村達男、小池和彦、脇田隆字、勝二郁夫、HCV コア蛋白に結合する新規宿主因子 hnRNPH1/H2 の HCV 生活環における役割、第31回日本分子生物学会年会、神戸、2008.

H. 知的所有権の出願・登録状況

なし

厚生労働科学研究費補助金（肝炎等克服緊急対策研究事業）
肝炎ウイルス感染の肝外病変の基礎的及び臨床的包括研究
分担研究報告書

HCV陽性者における末梢血Bリンパ球のclonality解析

研究分担者 岡村 孝 久留米大学血液内科 教授

研究要旨

HCV陽性者とコントロール群において、末梢血中にclonal（単一な、つまり腫瘍性の）なBリンパ球が存在する頻度をフローサイトメトリー（FCM）を用いて解析し、その細胞の特性について検討した。結果、clonalなBリンパ球のみられる症例はHCV陽性者に有意に多く存在することが示され、HCVがリンパ球をclonalに（腫瘍性に）増殖させる作用があることが示唆された。Clonalに増殖するBリンパ球のCD5発現は均一ではなく、これらの細胞はクローン内の多様性（intraclonal diversity）をもつ細胞集団であると考えられる。

A．研究目的

HCV陽性者における末梢血Bリンパ球のclonality（単一性、つまり腫瘍性）をフローサイトメトリー(FCM)を用いて解析する。さらに、clonalな増殖を示すB細胞の性状について精査することにより、HCVとリンパ増殖性疾患との関連について検討する。

B．研究方法

HCV(+)患者240例(インターフェロン治療、化学療法、免疫療法を施行中、また、リンパ系腫瘍、血液疾患を有する患者は除く)とコントロール（HCV(-)肝疾患患者）150例の末梢血リンパ球をCD19、κ、λの3種の抗体を用いて染色し､Bリンパ球のκ、λの発現比率を解析し、clonalityの有無を検討した。clonality陽性例では、CD5、CD20染色を追加し、免疫グロブリン重鎖遺伝子の再構成（IgH rearrangement）とBcl-2/IgH(t(14;18))転座の有無に関してPCR法を用いて検討した。

【検査内容、方法】

① 静脈採血（ヘパリン採血約5cc)を行い、適量を取り、洗浄して血漿を充分に除去する。CD19（Bリンパ球特異的マーカー)、κ、λの3種類の抗体を用いて染色した後、溶血剤により赤血球を除去する。充分に洗浄した後FCMを施行する。リンパ球領域をgatingし、CD19陽性集団内でのκ鎖、λ鎖の比率（κ/λ比）を算定する。κ/λ比3以上、1/2以下をclonality陽性とする。

② Clonality陽性例に関しては、CD19, CD5, CD20の3種類の抗体を用いて上記と同様の方法で染色する。FCMでリンパ球領域をgatingし、CD19陽性集団内でのCD5, CD20の発現を評価する。

③ 免疫グロブリン重鎖遺伝子の再構成に関しては、末梢血より単核球分離後、

DNA 採取を行い、primer を用いて semi-nested ＰＣＲを行い判定する。

④ Bcl-2/IgH (t(14;18))キメラ遺伝子に関しては、末梢血より単核球分離後、DNA 採取を行い、ＰＣＲを施行し、その有無を判定する。Bcl-2 には major breakpoint region (MBR) と minor cluster region (mcr) があり、それぞれに対して primer を作成し、ＰＣＲを行う。

(倫理面への配慮)

本研究は当大学の倫理委員会における承認を得ており、また、末梢血の提供者である患者には研究の意図を充分に説明し、文書で同意を得たうえで研究に参加していただいた。また、検体提供者の個人情報は確実に保護され、検体は上記検査目的のみに使用された。

C．研究結果

HCV(+)患者240例中7例にclonalなBリンパ球の増殖がみられたのに対し、コントロール (HCV(-)肝疾患患者) 150 例ではみられず、有意差あり ($p < 0.05$) の結果であった。7 例全てに IgH の monoclonal rearrangement が確認され、Bcl-2/IgH(t(14;18))転座は7例中1例で陽性であった。Clonal に増殖したBリンパ球のCD5発現強度は均一ではなく、正常の B リンパ球と比較して有意差は認めなかった。7 例中 2 例がインターフェロン治療をうけたが、2 例ともにclonalなBリンパ球の消失がみられた。

D．考察

本研究では、clonal なＢリンパ球の増殖がコントロール患者と比較して HCV(+)患者の末梢血において有意に多くみられることが示された。この事実は、HCV がリンパ球をclonal に(腫瘍性に)増殖させる作用があることを示唆する。さらに、HCV の消失と出現がclonalなBリンパ球の消失と再燃に並行する事実は、HCV とリンパ増殖性疾患との関係を強く示唆するものである。海外の論文ではPCR法を用いてHCV(+)患者の末梢血にclonalなBリンパ球が存在することは示されているが、その集団がＢリンパ球集団全体の中でどの程度を占めているかは検討されていない。われわれはフローサイトメトリー (FCM) を用いて同内容を検討した。結果、Ｂリンパ球数は正常範囲を維持しつつ、その中で clonal な腫瘍性Ｂリンパ球が大多数を占めていることが示された。

またHCV感染に伴うCD5陽性Bリンパ球の増減に関しては以前よりいくつかの報告があるが、見解は一致していない。そこで本研究では、HCV陽性者においてclonalに増殖することが確認されたＢリンパ球のCD5 発現に関して、正常リンパ球と比較しつつ検討した。結果、HCV関連のclonalなＢリンパ球は正常Ｂリンパ球と同様、個々の細胞によりそのCD5発現強度が異なり、また、CD5 陽性細胞の占める割合も正常 Ｂリンパ球と比較して有意差はないという事実が示された。これは、末梢血で増殖するHCV 関連 clonal Ｂリンパ球細胞は、'慢性リンパ性白血病細胞'(末梢血でclonalに増殖する、CD5 陽性細胞のみから構成される均一な細胞) とは異なる phenotype の細胞であることを示している。同じ clonal

なB細胞であっても分化段階において細胞表面形質（immunophenotype）が変化するという報告がある。本研究においてHCV関連clonal Bリンパ球細胞のCD5発現が均一でない点を考えると、これらのclonalなBリンパ球集団は分化段階の異なる種々の細胞の集合体である可能性が考えられる。

これらのHCV関連clonal Bリンパ球細胞が将来、悪性リンパ腫、クリオグロブリン血症などのリンパ増殖性疾患へと進展していくか否かに関して、今後の経時的観察が必要と考えられる。

E．結論

HCV(+)患者では末梢血Bリンパ球のclonalな（腫瘍性の）増殖がみられる症例が有意に多く存在する。そのCD5発現は均一ではなく、HCVにより増殖するBリンパ球はクローン内の多様性（intraclonal diversity)をもつ細胞集団であると考えられる。これらの細胞集団がリンパ増殖性疾患へと進展していくか否かについて今後の経時的研究が必要である。

F．研究発表

1．論文発表

1） 内藤嘉紀　久米徹　内藤雅康　橋口道俊岡村孝　江里口直文　内藤壽則　大島孝一　矢野博久　脾辺縁帯リンパ腫の1切除例 日本消化器外科学会雑誌 2008; 41: 229-234.

2．学会発表

1） 大坪維範　森重聡　奥英二郎　高田由香　関律子　今村理恵　橋口道俊　大崎浩一　薬師寺和昭　金地泰典　吉本幸治　岡村孝　川口巧　佐田通夫.　HCV陽性者における末梢血Bリンパ球のclonality解析.　第70回日本血液学会総会、京都、2008.

研究成果の刊行に関する一覧表

雑誌

発表者氏名	論文タイトル名	発表誌名	巻号	ページ	出版年
Tanaka N, Moriya K, Kiyosawa K, Koike K, Gonzalez FJ, Aoyama T.	PPAR-alpha is essential for severe hepatic steatosis and hepatocellular carcinoma induced by HCV core protein.	J Clin Invest	118	683-694	2008
Newell P, Villanueva A, Friedman SL, Koike K, Llovet JM.	Experimental models of hepatocellular carcinoma.	J Hepatol	48	858-879	2008
Koike K, Tsutsumi T, Miyoshi H, Shinzawa S, Shintani Y, Fujie H, Yotsuyanagi H, Moriya K.	Molecular Basis for the Synergy between Alcohol and Hepatitis C Virus in Hepatocarcinogenesis.	J Gastroenterol Hepatol	23	S87-91	2008
Ishizaka N, Ishizaka Y, Seki G, Nagai R, Yamakado M, Koike K.	Association between hepatitis B/C viral infection, chronic kidney disease and insulin resistance in individuals undergoing general health screening	Hepatol Res	38	775-783	2008
Nagase Y, Yotsuyanagi H, Okuse C, Yasuda K, Kato T, Koike K, Suzuki M, Nishioka K, Iino S, Itoh F.	Effect of treatment with interferon alpha-2b and ribavirin in patients infected with genotype 2 hepatitis C virus.	Hepatol Res	38	2522-258	2008
Koike K, Kikuchi Y, Kato M, Takamatsu J, Shintani Y, Tsutsumi T, Fujie H, Miyoshi H, Moriya K, Yotsuyanagi H.	Prevalence of Hepatitis B Virus Infection in Patients with Human Immunodeficiency Virus in Japan.	Hepatol Res	38	310-314	2008
Tanaka N, Moriya K, Kiyosawa K, Koike K, Aoyama T.	Hepatitis C virus core protein induces spontaneous and persistent activation of peroxisome proliferator-activated receptor alpha in transgenic mice: Implications for HCV-associated hepatocarcinogenesis.	Int J Cancer	122	124-131	2008
Ichibangase T, Moriya K, Koike K, Imai K.	Limitation of immunoaffinity column for the removal of abundant proteins from plasma in quantitative plasma proteomics.	Biomed Chromatogr		Nov 27. [Epub ahead of print]	2008

Ishizaka N, Ishizaka Y, Yamakado M, Toda E, Koike K, Nagai R.	Association between metabolic syndrome and carotid atherosclerosis in individuals without diabetes based on the oral glucose tolerance test.	Atherosclerosis		Oct 30. [Epub ahead of print]	2008
Koike K.	Steatosis, Liver Injury and Hepatocarcinogenesis in Hepatitis C Viral Infection.	J Gastroenterol	44	S82-88	2008
Mitsuyoshi H, Itoh Y, Sumida Y, Minami M, Yasui K, Nakashima T, Okanoue T.	Evidence of oxidative stress as a cofactor in the development of insulin resistance in patients with chronic hepatitis C.	Hepatol Res.	38	348-353	2008
Hiramatsu N, Kurashige N, Oze T, Takeraha T, Tamura S, Kasaraha A, Oshita M, Katayama K, Yoshihara H, Imai Y, Kato M, Kawata S, Tsubouchi H, Kumada H, Okanoue T, Kakumu S, Hayashi N.	Early decline of hemoglobin can predict progression of hemolytic anemia during pegylated interferon and ribavirin combination therapy in patients with chronic hepatitis C.	Hepatol Res	38	52-59	2008
Okanoue T, Itoh Y, Minami M, Hashimoto H, Yasui K, Yotsuyanagi H, Kumada T, Tanaka E, Nishiguchi S, Izumi N, Sata M, Onji M, Yamada G, Okita K, Kumada H.	Guidelines for the antiviral therapy of hepatitis C virus carriers with normal serum aminotransferase based on platelet counts.	Hepatol Res	38	27-36	2008
Zen K, Yasui K, Nakajima T, Zen Y, Zen K, Gen Y, Mitsuyoshi H, Minami M, Mitsufuji S, Tanaka S, Itoh Y, Nakanuma Y, Taniwaki M, Arii S, Okanoue T, Yoshikawa T.	ERK5 is a target for gene amplification at 17p11 and promotes cell growth in hepatocellular carcinoma by regulating mitotic entry.	Genes Chromosomes Cancer.	48	109-120	2009
Gen Y, Yasui K, Zen K, Nakajima T, Tsuji K, Endo M, Mitsuyoshi H, Minami M, Itoh Y, Tanaka S, Taniwaki M, Arii S, Okanoue T, Yoshikawa T.	A novel amplification target, ARHGAP5, promotes cell spreading and migration by negatively regulating RhoA in Huh-7 hepatocellular carcinoma cells.	Cancer Lett	275	27-34	2009
Mitsuyoshi H, Yasui K, Harano Y, Endo M, Tsuji K, Minami M, Itoh Y, Okanoue T.	Analysis of hepatic genes involved in the metabolism of fatty acids and iron in nonalcoholic fatty liver disease.	Hepatol Res		In press	2009

Akuta N, Suzuki F, Kawamura Y, Yatsuji H, Sezaki H, Suzuki Y, Hosaka T, Kobayashi M, Kobayashi M, Arase Y, Ikeda K, Kumada H.	Substitution of Amino Acid 70 in the Hepatitis C Virus Core Region of Genotype 1b Is an Important Predictor of Elevated Alpha-Fetoprotein in Patients Without Hepatocellular Carcinoma.	J Med Virol	80	1354-1362	2008
Akuta N, Suzuki F, Kawamura Y, Yatsuji H, Sezaki H, Suzuki Y, Hosaka T, Kobayashi M, Kobayashi M, Arase Y, Ikeda K, Kumada H.	Efficacy of Low-Dose Intermittent Interferon-Alpha Monotherapy in Patients Infected With Hwpatitis C Virus Genotype 1b Who Were Predicted or Failed to Respond to Pegylated Interferon Plus Ribavirin Combination Therapy.	J Med Virol	80	1363-1369	2008
Arase Y, Suzuki F, Sezaki H, Kawamura Y, Suzuki Y, Kobayashi M, Akuta N, Hosaka T, Yatsuji H, Hirakawa M, Kobayashi M, Ikeda K, Kumada H.	Efficacy in Patients with Dose Reduction in Combination Therapy of Peginterferon and Ribavirin for Chronic Hepatitis C.	Intervirology	51	1-6	2008
Arase Y, Suzuki F, Sezaki H, Kawamura Y, Suzuki Y, Kobayashi M, Akuta N, Hosaka T, Yatsuji H, Kobayashi M, Saitoh S, Ikeda K, Kumada H.	The Efficacy of Short-term Interferon-beta Therapy for Type C Cirrhotic Patients with Genotype 2a and Low Virus Load.	Intl Med	47	1085-1090	2008
Arase Y, Suzuki F, Sezaki H, Suzuki Y, Kawamura Y, Kobayashi M, Akuta N, Hosaka T, Yatsuji H, Ikeda K, Kobayashi M, Kumada H.	Suitable Treatment Period in patients with Virological Response during Combination Therapy of Pegonterferon and Ribavirin for Chroic Hepatitis C.	Int Med	47	1301-1307	2008
Arase Y, Suzuki F, Suzuki Y, Akuta N, Kobayashi M, Kawamura Y, Yatsuji H, Sezaki H, Hosaka T, Ikeda K, Kumada H.	Prolonged-Efficacy of Bisphosphonate in Postmenopausal Women With Osteoporosis and Chronic Liver Disease.	J Med Virol	80	1302-1307	2008
Arase Y, Suzuki F, Suzuki Y, Akuta N, Sezaki H, Kobayashi M, Kawamura Y, Yatsuji H, Hosaka T, Saitoh S, Ikeda K, Kumada H.	Potential of laparoscopy in chronic liver disease with hepatitis B and C viruses.	Hepatol Res	38	877-885	2008
Hirakawa M, Ikeda K, Kawamura Y, Kobayashi M, Hosaka T, Yatsuji H, Sezaki H, Akuta N, Suzuki F, Suzuki Y, Saitoh S, Arase Y, Kumada H.	New ablation procedure for a radiofrequency liver tissue coagulation sysytem using an expandable needle.	Liver International	28(2)	214-219	2008

Kobayashi M, Ikeda K, Arase Y, Suzuki Y, Suzuki F, Akuta N, Hosaka T, Murashima N, Saitoh S, Someya T, Tsubota A, Kumada H.	Inhibitory effect of branched-chain amino acid granules on progression of compensated liver cirrhosis due to hepatitis C virus.	J Gastroenterol	43	63-70	2008
Kawamura Y, Arase Y, Ikeda K, Suzuki F, Suziki Y, Kobayashi M, Akuta N, Hosaka T, Sezaki H, Yatsuji H, Kobayashi M, Kumada H.	The Efficacy of Short-term Interferon-beta Therapy for Chronic Hepatitis C Patients with Low Viurs Load.	Int Med	47	355-360	2008
Suzuki F, Suzuki Y, Akuta N, Yatsuji H, Sezaki H, Arase Y, Kawamura Y, Hosaka T, Kobayashi M, Ikeda K, Kobayashi M, Watahiki S, Kumada H.	Changes in viral loads of lamivudine-resistant mutants during entecavir therapy.	Hepatol Res	38	132-140	2008
Suzuki F, Toyoda J, Katano Y, Sata M, Moriyama M, Imazaki F, Kage M, Seriu T, Omata M, Kumada H.	Efficacy and safety of entecavir in lamivudine-refractory patients with chronic hepatitis B: Randomized controlled trial in Japanese patients.	J Gastrol Hepatol	29(9)	1-7	2008
Yatsuji H, Suzuki F, Sezaki H, Akuta N, Suziki Y, Kawamura Y, Hosaka T, Kobayashi M, Saitoh S, Arase Y, Ikeda K, Watahiki S, Iwasaki S, Kobayashi M, Kumada H.	Low risk of adefovir resisitance in lamivudine-resisitant chronic hepatitis B patients treated with adefovir plus lamibudine combination therapy: Two-year follow-up.	J Hepatol	48	923-931	2008
Hirakawa M, Ikeda K, Arase Y, Kawamura Y, Yatsuji H, Hosaka T, Sezaki H, Akuta N, Kobayashi M, Saitoh S, Suzuki F, Suzuki Y, Kumada H.	Hepatocarcinogenesis Following HCV RNA Eradication by Interferon in Chronic Hepatitis Patients.	Int Med	47	1637-1643	2008
Kasahara A, Kita K, Tomita E, Tyota J, Imai Y, Kumada H.	Repeated administration of recombinant human serum albumin caused no serious allergic reactions in patients with liver cirrhosis a multicenter clinical study.	J Gastroenterol	43	464-472	2008
Okanoue T, Itoh Y, Minami M, Hashimoto H, Yasui K, Yotsuyanagi H, Takehara T, Kumada T, Tanaka E, Nishiguchi s, Izumi N, Sata M, Onji M, Yamada G, Okita K, Kumada H.	Guidelines for the antiviral therapy of hepatitis C virus carriers with normal serum aminotransferase based on platelet counts.	Hepatol Res	38	27-36	2008

Yamada G, Iino S, Okuno T, Omata M, Kiyosawa K, Kumada H, Hayashi N, Sakai T.	Virologocal Response in Patients with Hepatitis C Virus Genotype 1b and a High Viral Load.	Clin Drug Invest	28, 1	9-16	2008
Hoshida Y, Villanueva A, Kobayashi M, Peix J, Chiang D, Camargo A, Gupta S, Moore J, Wrobel M, Lerner J, Reich M, Chan J, Glickman J, Ikeda K, Hashimoto M, Watanabe G, Daidone M, Roayaie S, Schwartz M, Thung S, Salvesen H, Gabriel S, Mazzaferro V, Bruix J, Friedman S, Kumada H, Llovet J, Golub T.	Gene Expression in Fixed tissues Outcome in Hepatocellular Carcinoma.	New England J Med	359(19)	1995-2004	2008
Katamura Y, Suzuki F, Akuta N, Sezaki H, Yatsuji H, Nomura H, Kawamura Y, Hosaka T, Kobayashi M, Suzuki Y, Saitoh S, Arase Y, Ikeda K, Kobayashi M, Kumada H.	Natural human interferon β plus rivavirin combination therapy in Japanese patients infected with hepatitis C virus and high viral load.	Internal Medicine	47	1827-2834	2008
Suzuki F, Miyakoshi H, Kobayashi M, Kumada H.	Correlation between Serum Hepatitis B Virus Core-Related Autigen and Intrahepatic Covalently Closed Circular DNA in Chronic Hepatitis B Patients.	J Med Virol	81	27-33	2008
Kobayashi M, Ikeda K, Arase Y, Suzuki F, Akuta N, Hosaka T, Sezaki H, Yatsuji H, Kobayashi M, Suzuki Y, Watahiki S, Mineta R, Iwasaki S, Miyakawa Y, Kumada H.	Change of Hepatitis B Virus Genotypes in Acute and Chronic Infections in Japan.	J Med Virol	80	1880-1884	2008
Sezaki H, Suzuki F, Kawamura Y, Yatsuji H, Hosaka T, Akuta N, Kobayashi M, Suzuki Y, Saitoh S, Arase Y, Ikeda K, Miyakawa Y, Kumada H.	Poor Response to Pegylated Interferon and Ribavirin in Aged Women Infected with Hepatitis C Virus of Genotype 1b in High Viral Loads.	Dig Dis Sci	in print	in print	2008
Arase Y, Suzuki F, Suzuki Y, Akuta N, Kobayashi M, Kawamura Y, Yatsuji H, Sezaki H, Hosaka T, Hirakawa M, Saitoh S, Ikeda K, Kobayashi M, Kumada H.	Sustained virological response reduces incidence of onset of type 2 diabetes in chronic hepatitis C.	Hepatology	49	1-6	2009

Furusyo N. Kajiwara E. Takahashi K. Nomura H. Tanabe Y. Masumoto A. Maruyama T. Nakamuta M. Enjoji M. Azuma K. Shimono J. Sakai H. Shimoda S. Hayashi J.	An association between the treatment length and cumrlative dose of pegylated interferon alpha-2b plus ribavirin and their effectiveness as a combination treatment for Japanese chronic hepatitis C patients: A project of the Kyushu University Liver Disease Study Group.	J Gastroenterol Hepatol	23	1094-1104	2008
林純、古庄憲浩、村田昌之.	院内で問題となる微生物と感染症－ウイルス感染症－	薬剤師のための感染制御標準テキスト		43-50	2008
林純、古庄憲浩、村田昌之、貝沼茂三郎、梶原英二.	インターフェロン無効のC型慢性肝炎に対する治療	学療法の領域	24 (2)	80-85	2008
林純、古庄憲浩、澤山泰典、村田昌之.	消化器病と動脈硬化症の病因としての感染症	福岡医学雑誌	99 (4)	67-73	2008
林純、古庄憲浩、梶原英二、中牟田誠、野村秀幸、高橋和弘、丸山俊博、増本陽秀、田邉雄一、遠城寺宗近.	C型慢性肝炎に対するインターフェロン療法	臨牀と研究	85 (7)	56-62	2008
林　純、古庄憲浩.	ウイルス感染症の現況と対策 HCV	臨牀と研究	85 (5)	695-700	2008
林純、古庄憲浩、小川栄一.	FibroScan の臨床的有用性について	臨牀と研究	85 (10)	148-152	2008
林純.	感染症としての肝炎	Medical ASAHI	37 (11)	78-80	2008
Daiju Fukuda, Masataka Sata, Nobukazu Ishizaka, Ryozo Nagai	Critical role of bone marrow angiotensin II type 1 receptor in the pathogenesis of atherosclerosis in apolipoprotein E deficient mice.	Arterioscler Thromb Vasc Biol	28(1)	90-96	2008

Nobukazu Ishizaka, Yuko Ishizaka, Ei-Ichi Toda, Kazuhiko Koike, Minoru Yamakado, Ryozo Nagai	Are serum carcinoembryonic antigen levels associated with carotid atherosclerosis in Japanese men?	Arterioscler Thromb Vasc Biol	28(1)	160-165	2008
Yasutomi Higashikuni, Nobukazu Ishizaka, Yuko Ishizaka, Ei-Ichi Toda, Ryozo Nagai, Minoru Yamakado	Relationship between blood pressure and chronic kidney disease in the Japanese population: the lower the better even in individuals without hypertension	Hypertension Res	31(2)	213-219	2008
Nobukazu Ishizaka, Yuko Ishizaka, Ei-Ichi Toda, Hiroji Shimomura, Kazuhiko Koike, George Seki, Ryozo Nagai, Minoru Yamakado	Association between cigarette smoking with chronic kidney disease in Japanese men.	Hypertension Res	31(3)	485-492	2008
Nobukazu Ishizaka, Yuko Ishizaka, George Seki, Ryozo Nagai, Minoru Yamakado, Kazuhiko Koike	Association between hepatitis B/C viral infection, chronic kidney disease and insulin resistance in individuals undergoing general health screening.	Hepatology Research	38(8)	775-783	2008
Yuko Ishizaka, Nobukazu Ishizaka, Mizuki Tani, Akiko Toda, Ei-Ichi Toda, Kazuhiko Koike, Minoru Yamakado	Relationship between albuminuria, low eGFR, and carotid atherosclerosis in Japanese women.	Kidney Blood Press Res	31(3)	164-170	2008
Gen Matsuzaki, Nobukazu Ishizaka, Kyoko Furuta, Makiko Hongo, Kan Saito, Ryota Sakurai, Kazuhiko Koike, Ryozo Nagai	Comparison of vasculoprotective effects of benidipine and losartan in a rat model of metabolic syndrome.	Eur J Pharmacol	587(1-3)	237-242	2008
Nobukazu Ishizaka, Yuko Ishizaka, Minoru Yamakado, Eiichi Toda, Kazuhiko Koike, Ryozo Nagai	Association between metabolic syndrome and carotid atherosclerosis in individuals without diabetes based on the oral glucose tolerance test.	Atherosclerosis	in press		2008
George Seki, Hideomi Yamada, Yuehong Lia,, Shoko Horita, Nobukazu Ishizaka, Kazuhiko Koike, Toshiro Fujita	Roles of MEK/ERK pathway in vascular and renal tubular actions of angiotensin II.	Vascular Disease Prevention	in press		2008
Makiko Hongo, Nobukazu Ishizaka, Kyoko Furuta, Naoya Yahagi, Kan Saito, Ryota Sakurai, Gen Matsuzaki, Kazuhiko Koike, Ryozo Nagai	Administration of angiotensin II, but not catecholamines, induces accumulation of lipids in the rat heart.	Eur J Pharmacol	604(1-3)	87-92	2009
Yuko Ishizaka, Nobukazu Ishizaka, Mizuki Tani, Akiko Toda, Ei-Ichi Toda, Kazuo Koike, Ryozo Nagai, Minoru Yamakado	Association between changes in obesity parameters and incidence of chronic kidney disease in Japanese individuals.	Kidney Blood Press Res	in press		2009

Okamoto K., Mori Y., Komoda Y., Okamoto T., Okochi M., Takeda M., Suzuki T., Moriishi K., and Matsuura Y.	Intramembrane processing by signal peptide peptidase regulates the membrane localization of hepatitis C virus core protein and viral propagation.	J. Virol.	82	8349-8361	2008
Masaki T., Suzuki R., Murakami K., Aizaki H., Ishii K., Murayama A., Date T., Matsuura Y., Miyamura T., Wakita T., and Suzuki T.	Interaction of hepatitis C virus nonstructural protein 5A with core protein is critical for the production of infectious virus particles.	J. Virol.	82	7964-7976	2008
Aizaki H., Morikawa K., Fukasawa M., Hara H., Inoue Y., Tani H., Saito K., Hanada K., Matsuura Y., Lai M. M. C., Miyamura T., Wakita T., and Suzuki T.	A critical role of virion-associated cholesterol and sphingolipid in hepatitis C virus infection.	J. Virol.	82	5715-5724	2008
Okamoto T., Omori H., Kaname Y., Abe T., Nishimura Y., Suzuki T., Miyamura T., Yoshimori T., Moriishi K., and Matsuura Y.	A single amino acid mutation in hepatitis C virus NS5A disrupting FKBP8 interaction impairs viral replication.	J. Virol.	82	3480-3489	2008
Taguwa S., Okamoto T., Abe T., Mori Y., Suzuki T., Moriishi K., and Matsuura Y.	Human butyrate-induced transcript 1 interacts with hepatitis C virus NS5A and regulates viral replication.	J. Virol.	82	2631-2641	2008
Murakami, K., Inoue, Y., Hmwe, S. S., Omata, K., Hongo, T., Ishii, K., Yoshizaki, S., Aizaki, H., Matsuura, T., Shoji, I., Miyamura, T., and Suzuki, T.	Dynamic behavior of hepatitis C virus quasispecies in a long-term culture of the three-dimensional radial-flow bioreactor system.	*Journal of Virological Methods*	148	174-181	2008
Murakami, K., Kimura, T., Osaki, M., Ishii, K., Miyamura, T., Suzuki, T., Wakita, T., and Shoji, I.	Virological characterization of the HCV JFH-1 strain in lymphocytic cell lines.	*Journal of General Virology*	89	1587-92	2008
Sasase, N., Kim, S. R., Kim, K. I., Taniguchi, M., Imoto, S., Mita, K., Hotta, H., Shoji, I., El-Shamy, A., Kawada, N., Kudo, M., and Hayashi, Y.	Usefulness of a new immunoradiometric assay of HCV core antigen to predict virological response during PEG-IFN/RBV combination therapy for chronic hepatitis with high viral load of serum HCV RNA genotype 1b.	*Intervirology*	51	70-75	2008
Deng, L., Adachi, T., Kitayama, K., Bungyoku, Y., Kitazawa, S., Ishido, S., Shoji, I., and Hotta, H.	Hepatitis C virus infection induces apoptosis through a Bax-triggered, mitochondria-mediated, Caspase-3-dependent pathway.	*Journal of Virology*	82	10375-85	2008

Suzuki, R., Moriishi, K., Fukuda, K., Shirakura, M., Ishii, K., Shoji, I., Wakita, T., Miyamura, T., Matsuura, Y., and Suzuki, T.	Proteasomal turnover of hepatitis C virus core protein is regulated by dual mechanisms, ubiquitin-dependent and ubiquitin-independent but PA28gamma-dependent.	*Journal of Virology*	[epub ahead of print]		2008
Shimoji, T., Murakami, K., Sugiyama, Y., Matsuda, M., Inubushi, S., Nasu, J., Shirakura, M., Suzuki, T., Wakita, T., Kishino, T., Hotta, H., Miyamura, T., and Shoji, I.	Identification of annexin A1 as a novel substrate for E6AP-mediated ubiquitylation.	*Journal of Cellular Biochemistry*	in press		2009
金守良、井本勉、婦木秀一、金啓二、谷口美幸、長野基子、堀田博、勝二郁夫、寒原芳浩、前川陽子、工藤正俊、林祥剛.	1b型高ウイルス量高齢者C型慢性肝炎に対するPEG IFNα-2b/リバビリン治療（併用療法）の検討.	肝臓	49	145-152	2008
S. Yamaguchi, H. Ishihara, T. Yamada, A. Tamura, M. Usui, R. Tominaga, Y. Munakata, C. Satake, H. Katagiri, F. Tashiro, H. Aburatani, K. Tsukiyama-Kohara, J. Miyazaki, N. Sonenberg and Y. Oka.	ATF4-Mediated Induction of 4E-BP1 Contributes to Pancreatic β Cell Survival under Endoplasmic Reticulum Stress.	*Cell Metabolism*	7(3)	269-276	2008
T. Nishimura, M. Saito, T. Takano, A. Nomoto, M. Kohara, and K. Tsukiyama-Kohara.	Comparative Aspects on the Role of Polypyrimidine Tract Binding Protein in Internal Initiation of Hepatitis C Virus and Picornavirus RNAs.	*Comp. Immunol. Microbiol. Infect. Dis.*	5	435-448	2008
H. Sato, R. Honma, M. Yoneda, R. Miura, K. Tsukiyama-Kohara, F. Ikeda, T. Seki, S. Watanabe, and C. Kai.	Measles virus induces cell-type specific changes in gene expression.	*Virology*	375 (2)	321-330	2008
Y. Terao-Muto, M. Yoneda, T. Seki, A. Watanabe, K. Tsukiyama-Kohara, K. Fujita, and C. Kai.	Heparin-like glycosaminoglycans prevent the infection of measles virus in SLAM-negative cell lines.	*Antiviral Res.*	80(3)	370-376	2008
Y. Inoue, K. Tsukiyama-Kohara, M. Yoneda, H. Sato, and C. Kai.	Inhibition of host protein synthesis in B95a cells infected with the HL strain of measles virus.	*Comp Immunol Microbiol Infect Dis*	32(1)	29-41	2009
内藤嘉紀　久米徹　内藤雅康　橋口道俊　岡村孝　江里口直文　内藤壽則　大島孝一　矢野博久	脾辺縁帯リンパ腫の1切除例	日本消化器外科学会雑誌	41	229-234	2008

PPARα activation is essential for HCV core protein–induced hepatic steatosis and hepatocellular carcinoma in mice

Naoki Tanaka,[1,2] Kyoji Moriya,[3] Kendo Kiyosawa,[2] Kazuhiko Koike,[3] Frank J. Gonzalez,[4] and Toshifumi Aoyama[1]

[1]Department of Metabolic Regulation, Institute on Aging and Adaptation, Shinshu University Graduate School of Medicine, Matsumoto, Nagano, Japan.
[2]Division of Gastroenterology, Department of Internal Medicine, Shinshu University School of Medicine, Matsumoto, Nagano, Japan.
[3]Department of Infectious Diseases, Internal Medicine, Graduate School of Medicine, University of Tokyo, Tokyo, Japan.
[4]Laboratory of Metabolism, National Cancer Institute, NIH, Bethesda, Maryland, USA.

Transgenic mice expressing HCV core protein develop hepatic steatosis and hepatocellular carcinoma (HCC), but the mechanism underlying this process remains unclear. Because PPARα is a central regulator of triglyceride homeostasis and mediates hepatocarcinogenesis in rodents, we determined whether PPARα contributes to HCV core protein–induced diseases. We generated PPARα-homozygous, -heterozygous, and -null mice with liver-specific transgenic expression of the core protein gene (*Ppara*$^{+/+}$:HCVcpTg, *Ppara*$^{+/-}$:HCVcpTg, and *Ppara*$^{-/-}$:HCVcpTg mice. Severe steatosis was unexpectedly observed only in *Ppara*$^{+/+}$:HCVcpTg mice, which resulted from enhanced fatty acid uptake and decreased mitochondrial β-oxidation due to breakdown of mitochondrial outer membranes. Interestingly, HCC developed in approximately 35% of 24-month-old *Ppara*$^{+/+}$:HCVcpTg mice, but tumors were not observed in the other genotypes. These phenomena were found to be closely associated with sustained PPARα activation. In *Ppara*$^{+/-}$:HCVcpTg mice, PPARα activation and the related changes did not occur despite the presence of a functional *Ppara* allele. However, long-term treatment of these mice with clofibrate, a PPARα activator, induced HCC with mitochondrial abnormalities and hepatic steatosis. Thus, our results indicate that persistent activation of PPARα is essential for the pathogenesis of hepatic steatosis and HCC induced by HCV infection.

Introduction

HCV is one of the major causes of chronic hepatitis, whereas patients with persistent HCV infection have a high incidence of hepatocellular carcinoma (HCC) (1, 2). Occurrence of HCC associated with chronic HCV infection has increased over the past 2 decades (3–5), and chronic HCV infection is recognized as a serious debilitating disease. However, the mechanism in which chronic HCV infection mediates hepatocarcinogenesis remains unclear.

HCV core protein was shown to have oncogenic potential (6). To examine how HCV core protein participates in HCV-related hepatocarcinogenesis, transgenic mouse lines were established in which HCV core protein is expressed constitutively in liver at cellular levels similar to those found in chronic HCV-infected patients (7). These mice exhibited hepatic steatosis (7) and insulin resistance (8) as early as 3 months of age; on further aging, these symptoms worsened and hepatic adenomas developed in approximately 30% of mice between 16 and 18 months of age (9). Finally, HCC was found within hepatic adenomas in a classic "nodule-in-nodule" pathology (9). Interestingly, no hepatic inflammation or fibrosis was found in these mice throughout the course of HCC development (9), which suggested that the HCV core protein itself induces hepatic steatosis and HCC independently of hepatitis.

Several studies support the contention that hepatic steatosis promotes the development of HCC (10). Epidemiologic data have identified hepatic steatosis as a major accelerating factor of hepatocarcinogenesis in chronic HCV-infected patients (11). Moreover, increases in ROS production that can cause oxidative DNA damage, mitochondrial abnormalities, and accelerated hepatocyte proliferation were observed in the steatotic livers (12–14). Thus, an intriguing possibility has emerged that alteration of fatty acid metabolism in hepatocytes may be central to the pathogenesis of HCC induced by HCV core protein.

PPARs are ligand-activated nuclear receptors belonging to the steroid/thyroid hormone receptor superfamily; 3 isoforms designated as α, β/δ, and γ exist, all of which are involved in lipid homeostasis (15). PPARα regulates constitutive transcription of genes encoding fatty acid–metabolizing enzymes (16) and is associated with the maintenance of fatty acid transport and metabolism, primarily in liver, kidney, and heart. Administration of PPARα agonists, such as the widely prescribed fibrate drugs clofibrate, gemfibrozil, and fenofibrate, ameliorate hyperlipidemia in humans (17) and hepatic steatosis in mice (18).

On the other hand, long-term administration of PPARα ligands to rodents causes accelerated hepatocyte proliferation, increased ROS generation, and development of HCC (19, 20). Disruption of the PPARα gene was shown to prevent the development of HCC caused by long-term exposure to PPARα activators (21). Interestingly, accumulation of fatty acids/triglycerides in hepatocytes

Nonstandard abbreviations used: ACC, acetyl-CoA carboxylase; AOX, acyl-CoA oxidase; CDK, cyclin-dependent kinase; CYP4A1, cytochrome P450 4A1; FAS, fatty acid synthase; FAT, fatty acid translocase; FATP, fatty acid transport protein; HCC, hepatocellular carcinoma; HCVcpTg, HCV core protein–expressing transgenic; L-FABP, liver fatty acid-binding protein; MCAD, medium-chain acyl-CoA dehydrogenase; MTP, microsomal transfer protein; 8-OHdG, 8-hydroxy-2′-deoxyguanosine; PCNA, proliferating cell nuclear antigen; RXRα, retinoid X receptor α.

Conflict of interest: The authors have declared that no conflict of interest exists.

Citation for this article: *J. Clin. Invest.* **118**:683–694 (2008). doi:10.1172/JCI33594.

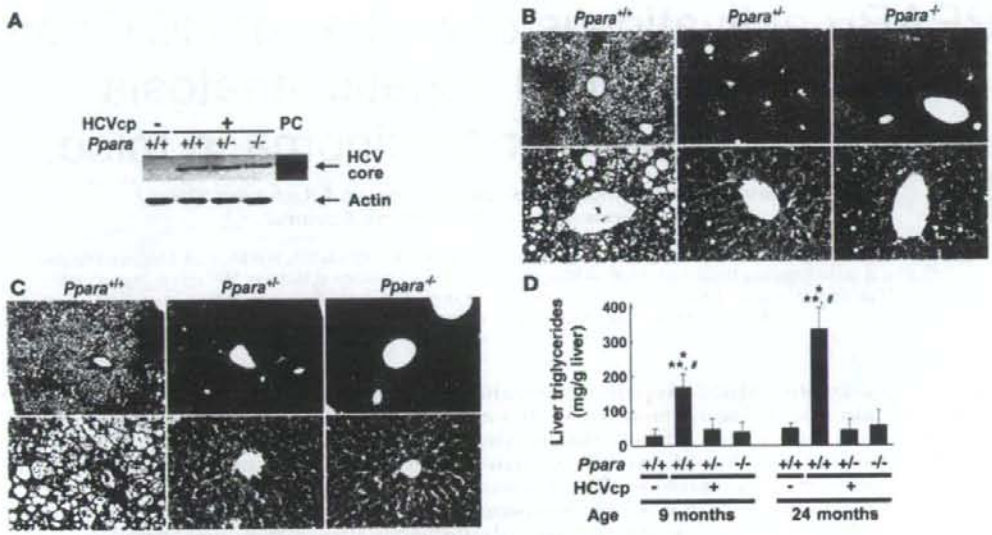

Figure 1

Phenotype changes in transgenic mouse liver. (**A**) Immunoblot analysis of HCV core protein expression in livers of 9-month-old mice. Because no significant individual differences in the same mouse group were found in the preliminary experiments, 10 mg of liver prepared from each mouse ($n = 6$/group) was mixed and homogenized. Whole-liver lysate (50 μg protein) was loaded in each well. The band of actin was used as the loading control. Results are representative of 4 independent experiments. PC, lysate prepared from COS-1 cells overexpressing HCV core protein as a positive control. (**B**) Histological appearance of hematoxylin- and eosin-stained liver sections from 9-month-old HCVcpTg mice. Upper and lower rows show a lower (×40) and higher (×400) magnification, respectively. Microvesicular and macrovesicular steatosis was found only in *Ppara*$^{+/+}$:HCVcpTg mice. No inflammation or hepatocyte degeneration was evident in any of the genotypes. (**C**) Histological appearance of hematoxylin- and eosin-stained liver sections from 24-month-old HCVcpTg mice. Upper and lower rows show a lower (×40) and higher (×400) magnification, respectively. Hepatic steatosis was marked in *Ppara*$^{+/+}$:HCVcpTg mice, but not in other mice. Hepatic inflammation, fibrosis, and hepatocyte degeneration were not observed. In *Ppara*$^{+/-}$:HCVcpTg and *Ppara*$^{-/-}$:HCVcpTg mice, dysplastic hepatocytes and precancerous lesions were not detected throughout the entire liver. (**D**) Content of liver triglycerides. Results are expressed as the mean ± SD ($n = 6$/group) and compared between genotypes at the same age. $^{*}P < 0.05$ compared with *Ppara*$^{+/+}$ nontransgenic mice; $^{**}P < 0.05$ compared with *Ppara*$^{+/-}$:HCVcpTg mice; $^{\#}P < 0.05$ compared with *Ppara*$^{-/-}$:HCVcpTg mice.

could lead to continuous PPARα activation because of the presence of fatty acid metabolites that serve as natural PPARα ligands. For example, mice lacking expression of the peroxisomal acyl-CoA oxidase (AOX) gene showed massive accumulation of very-long-chain fatty acids in hepatocytes, severe microvesicular steatosis, chronic PPARα activation, and development of hepatic adenoma and HCC by 15 months of age (22). These results suggest a strong contribution of activated PPARα to liver tumorigenesis.

On the basis of several lines of evidence, we hypothesized that PPARα might contribute to hepatocarcinogenesis in HCV core protein–expressing transgenic (HCVcpTg) mice. To explore this possibility, PPARα-homozygous (*Ppara*$^{+/+}$), PPARα-heterozygous (*Ppara*$^{+/-}$), and PPARα-null (*Ppara*$^{-/-}$) mice bearing the HCV core protein gene, designated *Ppara*$^{+/+}$:HCVcpTg, *Ppara*$^{+/-}$:HCVcpTg, and *Ppara*$^{-/-}$:HCVcpTg mice, were generated, and phenotypic changes were examined. Surprisingly, we found that severe hepatic steatosis and HCC induced by HCV core protein developed only in *Ppara*$^{+/+}$ mice, which were related to persistent PPARα activation.

Results

Expression of HCV core protein in transgenic mice. *Ppara*$^{-/-}$:HCVcpTg and *Ppara*$^{+/-}$:HCVcpTg mice appeared healthy, and body weight in both genotypes was similar to that of *Ppara*$^{+/+}$:HCVcpTg and *Ppara*$^{+/+}$ mice without the transgene. When hepatic expression of HCV core protein in 9-month-old transgenic mice was examined by immunoblot analysis, it was similar among *Ppara*$^{+/+}$:HCVcpTg, *Ppara*$^{+/-}$:HCVcpTg, and *Ppara*$^{-/-}$:HCVcpTg mice (Figure 1A) and was also similar to expression in HCVcpTg mice reported previously (7, 9). Age and sex had only a minor influence on the hepatic expression of HCV core protein.

Requirement of homozygous PPARα for the development of hepatic steatosis in transgenic mice. Livers of 9-month-old male HCVcpTg mice with or without the *Ppara* allele were examined. Those of *Ppara*$^{+/+}$:HCVcpTg mice were soft, slightly enlarged, and light in color and histologically showed macrovesicular and microvesicular steatosis with no apparent inflammation or hepatocyte necrosis (Figure 1B), in agreement with previous reports (7, 9). Biochemical analysis of liver extracts showed marked hepatic accumulation of triglycerides (Figure 1D). In contrast, livers of 9-month-old *Ppara*$^{+/-}$:HCVcpTg and *Ppara*$^{-/-}$:HCVcpTg mice showed neither histological abnormalities nor accumulation of triglycerides (Figure 1, B and D). Hepatic levels of free fatty acids in *Ppara*$^{+/+}$:HCVcpTg mice were approximately 3 times those in *Ppara*$^{+/-}$:HCVcpTg and *Ppara*$^{-/-}$:HCVcpTg mice or *Ppara*$^{+/+}$ mice not expressing the HCV core protein.

In 24-month-old *Ppara*$^{+/+}$:HCVcpTg mice, hepatic steatosis was found (Figure 1C), and the hepatic levels of triglycerides were further increased (Figure 1D). Apparent inflammation, hepatocyte

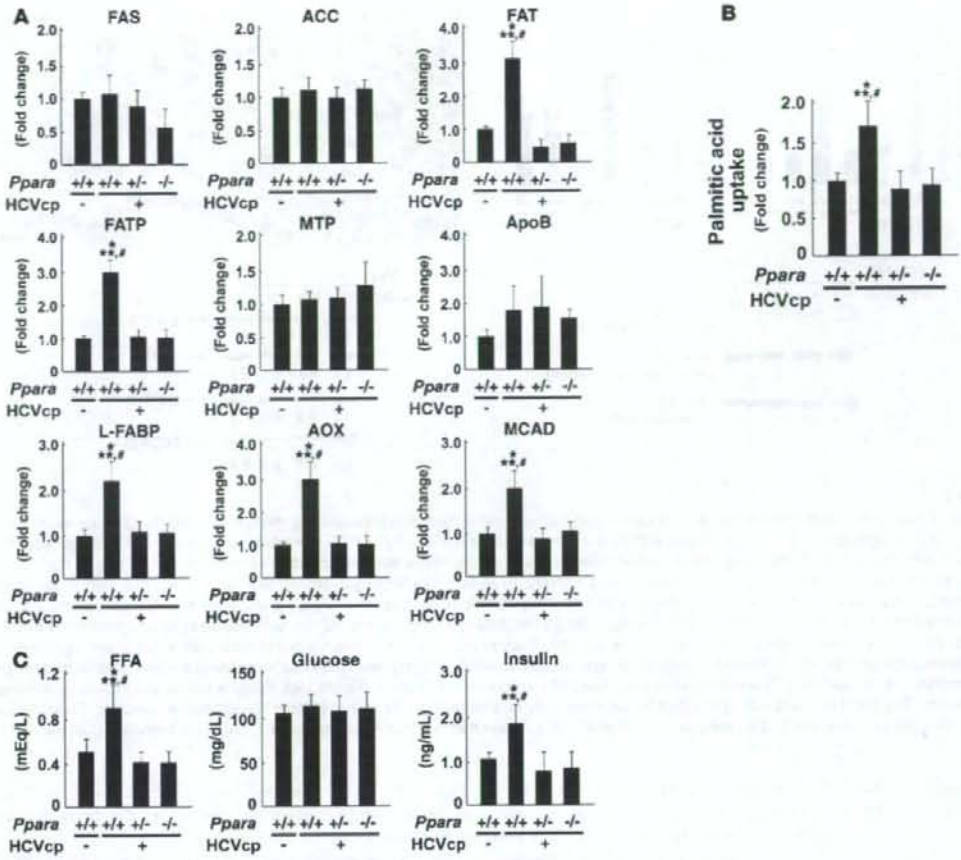

Figure 2

Analyses of factors associated with hepatic fatty acid and triglyceride metabolism. (**A**) Expression of genes associated with fatty acid and triglyceride metabolism in 9-month-old mouse livers. Total RNA was extracted from each mouse liver, and mRNA levels were determined by RT-PCR. mRNA levels were normalized by those of GAPDH and subsequently normalized by those in *Ppara*$^{+/+}$ nontransgenic mice. Results are expressed as the mean ± SD (n = 6/group). *P < 0.05 compared with *Ppara*$^{+/+}$ nontransgenic mice; **P < 0.05 compared with *Ppara*$^{+/-}$:HCVcpTg mice; #P < 0.05 compared with *Ppara*$^{-/-}$:HCVcpTg mice. (**B**) Uptake of fatty acids in 9-month-old mouse livers. Liver slices obtained from 3 mice in each group were incubated in medium containing 0.8 mM [1-^{14}C]palmitic acid for 7 h. Fatty acid uptake ability was estimated by the sum of palmitic acid converted to CO_2 and ketone bodies with that incorporated into total cellular lipids after incubation. The experiment was repeated 3 times. Results were normalized by those of *Ppara*$^{+/+}$ nontransgenic mice and expressed as the mean ± SD. (**C**) Plasma concentrations of free fatty acids, glucose, and insulin. After an overnight fast, blood was obtained from each mouse and the above variables were determined. Results are expressed as the mean ± SD (n = 6/group).

degeneration and necrosis, and fibrosis were not detected. On the other hand, *Ppara*$^{+/-}$:HCVcpTg and *Ppara*$^{-/-}$:HCVcpTg mice showed no steatosis (Figure 1, C and D). These results indicate that hepatic steatosis develops in *Ppara*$^{+/+}$:HCVcpTg mice, but not in *Ppara*$^{+/-}$:HCVcpTg and *Ppara*$^{-/-}$:HCVcpTg mice.

Hepatic fatty acid and triglyceride metabolism in transgenic mice. To investigate the mechanism responsible for the development of severe steatosis in *Ppara*$^{+/+}$:HCVcpTg mice, the expression of genes associated with fatty acid and triglyceride metabolism in the livers of 9-month-old mice was analyzed using the quantitative RT-PCR method. As shown in Figure 2A, the mRNA levels of genes related to de novo lipogenesis (fatty acid synthase [FAS] and acetyl-CoA carboxylase [ACC]) and secretion of VLDL (microsomal transfer protein [MTP] and apoB) were constant in all groups. The mRNA levels of fatty acid translocase (FAT) and fatty acid transport protein (FATP), which are associated with the uptake of fatty acids into hepatocytes, were significantly increased only in *Ppara*$^{+/+}$:HCVcpTg mice, but the mRNA levels of hepatic triglyceride lipase, another contributor to fatty acid uptake, remained unchanged (data not shown). The mRNA levels of liver fatty acid binding protein (L-FABP) were also elevated only in *Ppara*$^{+/+}$:HCVcpTg mice. Surprisingly, the mRNA levels of AOX and medium-chain acyl-CoA

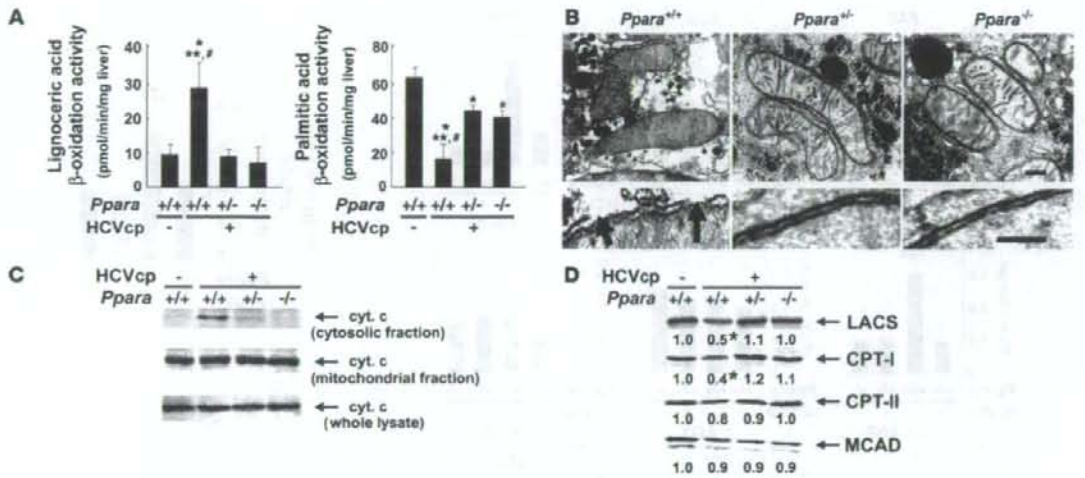

Figure 3

Analyses of mitochondrial abnormalities. (**A**) Lignoceric and palmitic acid β-oxidation activities in 9-month-old mice. Results are expressed as the mean ± SD (n = 6/group). *P < 0.05 compared with *Ppara*$^{+/+}$ nontransgenic mice; **P < 0.05 compared with *Ppara*$^{+/-}$:HCVcpTg mice; #P < 0.05 compared with *Ppara*$^{-/-}$:HCVcpTg mice. (**B**) Electron microscopic features of hepatic mitochondria of 9-month-old HCVcpTg mice. Upper and lower rows show a lower and higher magnification, respectively. In *Ppara*$^{+/+}$:HCVcpTg mice, some mitochondria showing discontinuance of outer membranes (arrows) and amorphous inner structures were observed. In *Ppara*$^{+/-}$:HCVcpTg and *Ppara*$^{-/-}$:HCVcpTg mice, mitochondria appeared normal; the scale bars represent 200 nm (top) and 30 nm (bottom), respectively. (**C**) Immunoblot analysis of cytochrome *c* in 9-month-old mice. Whole-liver lysate, mitochondrial fraction, or cytosolic fraction (50 μg protein) was loaded in each well. Results are representative of 4 independent experiments. (**D**) Immunoblot analysis of representative mitochondrial β-oxidation enzymes using a mitochondrial fraction prepared from 9-month-old mouse livers. The mitochondrial fraction (20 μg protein) was loaded in each well. Results are representative of 4 independent experiments. The band intensity was quantified densitometrically and normalized by that in *Ppara*$^{+/+}$ nontransgenic mouse. The mean value of the fold changes is shown under the representative band. LACS, long-chain acyl-CoA synthase; CPT, carnitine palmitoyl-CoA transferase.

dehydrogenase (MCAD), a rate-limiting enzymes in the peroxisomal and mitochondrial β-oxidation pathways, respectively, were significantly increased in *Ppara*$^{+/+}$:HCVcpTg mice. When fatty acid uptake ability was measured in fresh liver slices, it was significantly enhanced only in *Ppara*$^{+/+}$:HCVcpTg mice (Figure 2B). Additionally, plasma free fatty acid levels were higher in these mice than in mice in the other groups. Although there were no differences in fasting plasma glucose levels between the groups, hyperinsulinemia was observed only in *Ppara*$^{+/+}$:HCVcpTg mice (Figure 2C), in agreement with the previous observation that significant insulin resistance developed in these mice (8). Similar results were obtained from 24-month-old mice (data not shown). These results combined show that the increased plasma fatty acid levels, which were likely due to enhanced peripheral fatty acid release caused by insulin resistance, and the increase in fatty acid uptake ability are consistent with steatogenesis in *Ppara*$^{+/+}$:HCVcpTg mice.

Decreased mitochondrial β-oxidation in transgenic mice. Although the transcriptional activities of major β-oxidation enzymes were markedly increased, *Ppara*$^{+/+}$:HCVcpTg mice had severe steatosis. To explore this discrepant result, peroxisomal and mitochondrial β-oxidation activities were measured using lignoceric and palmitic acids as substrates, respectively. The lignoceric acid–degrading capacity was increased only in *Ppara*$^{+/+}$:HCVcpTg mice, where it corresponded to an increase in AOX expression. However, the capacity for palmitic acid degradation, which occurs particularly in mitochondria, was significantly lower in *Ppara*$^{+/+}$:HCVcpTg mice than in *Ppara*$^{+/-}$:HCVcpTg and *Ppara*$^{-/-}$:HCVcpTg mice (Figure 3A). Thus, decreased mitochondrial β-oxidation ability was considered to be another important mechanism for the development of steatosis induced by the core protein.

We further evaluated mitochondrial abnormalities. In electron microscopic examination, discontinuous outer membranes (Figure 3B, arrows) and lack of an internal structure were observed in some mitochondria of *Ppara*$^{+/+}$:HCVcpTg mouse livers, in agreement with the previous report (9). However, these abnormalities were not seen in *Ppara*$^{+/-}$:HCVcpTg and *Ppara*$^{-/-}$:HCVcpTg mice (Figure 3B). Immunoblot analysis showed that cytochrome *c*, which is usually localized in the mitochondrial intermembrane space, was present in the cytosolic fractions of *Ppara*$^{+/+}$:HCVcpTg mice (Figure 3C). Moreover, immunoblot analysis using mitochondrial fractions showed that the expression levels of long-chain acyl-CoA synthase and carnitine palmitoyl-CoA transferase-I, which are enzymes indispensable to the initial step of mitochondrial β-oxidation and are localized mainly in mitochondrial outer membranes, were significantly decreased only in *Ppara*$^{+/+}$:HCVcpTg mice (Figure 3D).

Overall, these results suggest that homozygous PPARα is essential to the pathogenesis of hepatic steatosis induced by the HCV core protein, which results from a decrease in mitochondrial fatty acid degradation capacity caused by the breakdown of mitochondrial outer membranes and a disproportionate increase in the uptake of fatty acids. Interestingly, steatosis and the related changes did not occur in *Ppara*$^{+/-}$ and *Ppara*$^{-/-}$ mice expressing the HCV core protein, which suggested that these changes were not caused by the core protein itself.

Table 1
Incidence of HCC in 24-month-old mice

HCV core protein	*Ppara*	Mice (*n*)	Mice with HCC (*n*)	Incidence (%)
–	+/+	20	0	0
–	+/–	18	0	0
–	–/–	20	0	0
+	+/+	17	6	35.3[A]
+	+/–	16	0	0
+	–/–	14	0	0

Mice were killed at 24 months of age for analysis. HCC was diagnosed according to histological findings. [A]$P < 0.05$ compared with *Ppara*$^{+/+}$ nontransgenic mice, $P < 0.05$ compared with *Ppara*$^{+/-}$:HCVcpTg mice, $P < 0.05$ compared with *Ppara*$^{-/-}$:HCVcpTg mice.

Requirement of homozygous PPARα for hepatic tumor development in transgenic mice. At 9 months of age, hepatic nodules were not observed at all in transgenic mice, whereas, at 24 months, approximately 35% of *Ppara*$^{+/+}$:HCVcpTg mice had macroscopically evident hepatic nodules (Table 1). Microscopically, these nodules had the appearance of well-differentiated HCC with trabecular features, which was consistent with the previous report (9). Surprisingly, *Ppara*$^{+/-}$:HCVcpTg and *Ppara*$^{-/-}$:HCVcpTg mice of the same ages developed no evidence of hepatic tumors, despite the expression of HCV core protein at similar levels to those found in *Ppara*$^{+/+}$:HCVcpTg mice (Table 1). Microscopic examination showed that there were no dysplastic cells or precancerous lesions throughout the livers in *Ppara*$^{+/-}$:HCVcpTg and *Ppara*$^{-/-}$:HCVcpTg mice (Figure 1C). These results provide strong evidence that homozygous PPARα is essential for hepatic tumorigenesis induced by HCV core protein.

Increased hepatocyte proliferation only in Ppara$^{+/+}$*:HCVcpTg mice.* Because sustained acceleration of hepatocyte proliferation relative to apoptosis may promote the development of HCC, these opposing processes were quantified in the livers of 24-month-old mice. Both the liver-to-body weight ratio and the number of hepatocytes expressing proliferating cell nuclear antigen (PCNA) were increased only in *Ppara*$^{+/+}$:HCVcpTg mice (Figure 4, A and B). In contrast, the number of TUNEL-positive hepatocytes and the hepatic caspase 3 activity, indicators of hepatocyte apoptosis, remained similar among the 3 mouse strains (Figure 4, C and D). Interestingly, despite the presence of HCV core protein, the amounts of these proliferative and apoptotic markers in *Ppara*$^{+/-}$:HCVcpTg and *Ppara*$^{-/-}$:HCVcpTg mice were similar to those in *Ppara*$^{+/+}$ nontransgenic mice. Expression levels of several proteins, such as protooncogenes (c-Fos and c-Myc), cell-cycle regulators (cyclin D1, cyclin-dependent kinase [CDK] 4, and PCNA), and phosphorylated ERK 1 and 2, all of which are associated with hepatocyte proliferation, were elevated in *Ppara*$^{+/+}$:HCVcpTg mice but not in other genotypes (Figure 4, E and F).

Increased oxidative stress and DNA damage only in Ppara$^{+/+}$*:HCVcpTg mice.* HCV core protein is associated with increased production of ROS (23). Enhanced ROS production induces nuclear DNA damage, which results in the initiation of hepatocarcinogenesis, and can also injure organelles, which can result in disorders in their

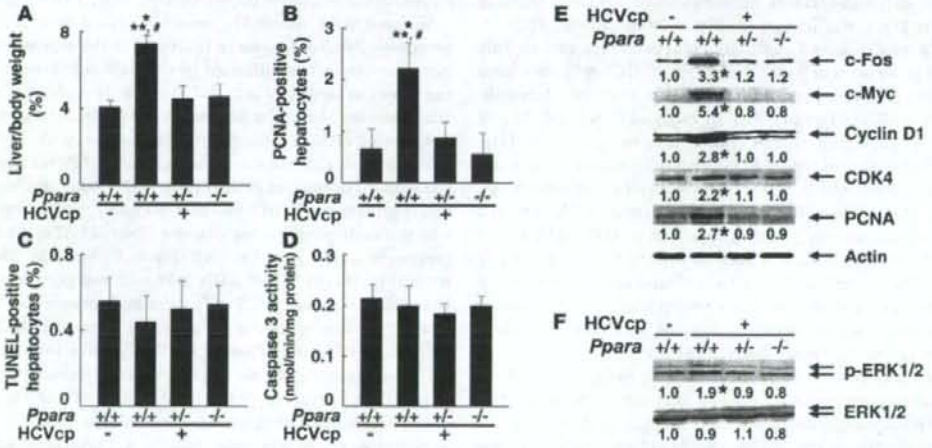

Figure 4
Increased hepatocyte proliferation in *Ppara*$^{+/+}$:HCVcpTg mice at 24 months of age. (**A**) Liver-to-body-weight ratio. Results are expressed as the mean ± SD (n = 6/group). (**B**) Numbers of proliferating hepatocytes. Two thousand hepatocytes were examined in each mouse, and hepatocyte nuclei positive for anti-PCNA antibody were counted. Results are expressed as the mean ± SD (n = 6/group). For **A** and **B**, comparisons are designated as follows: *$P < 0.05$ compared with *Ppara*$^{+/+}$ nontransgenic mice; **$P < 0.05$ compared with *Ppara*$^{+/-}$:HCVcpTg mice; #$P < 0.05$ compared with *Ppara*$^{-/-}$:HCVcpTg mice. (**C**) Numbers of apoptotic hepatocytes. Liver sections were subjected to TUNEL staining, and TUNEL-positive hepatocyte nuclei were counted in 2,000 hepatocytes from each mouse. Results are expressed as the mean ± SD (n = 6/group). (**D**) Caspase 3 activity. Results are expressed as the mean ± SD (n = 6/group). (**E**) Immunoblot analysis of oncogene products and cell cycle regulators. The same sample used in Figure 1A (whole-liver lysate, 50 μg protein) was loaded in each well. The band of actin was used as the loading control. Results are representative of 4 independent experiments. The band intensity was quantified densitometrically, normalized by that of actin, and subsequently normalized by that in *Ppara*$^{+/+}$ nontransgenic mice. The mean value of the fold changes is expressed under each band. (**F**) Immunoblot analysis of phosphorylated ERK1/2 and total ERK1/2. The same samples in Figure 4E (50 μg protein) were used.

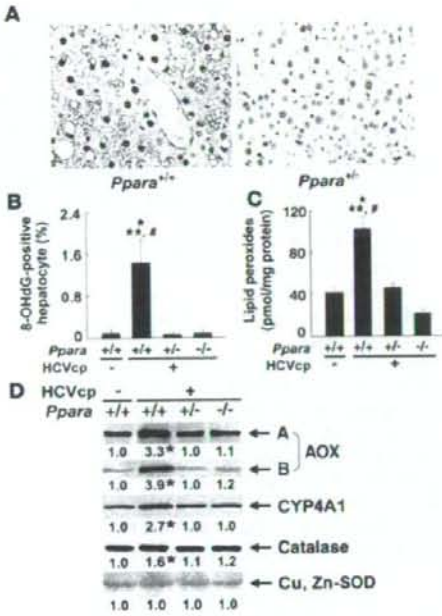

Figure 5
Increased oxidative stress and DNA damage in *Ppara*$^{+/+}$:HCVcpTg mice at 24 months of age. (**A**) Immunohistochemical staining using antibody against 8-OHdG. In *Ppara*$^{+/+}$:HCVcpTg mice, some steatotic hepatocytes were positive for 8-OHdG. Original magnification, ×400. (**B**) Numbers of 8-OHdG–positive hepatocytes. Hepatocyte nuclei stained with anti-8-OHdG antibody were counted in 2,000 hepatocytes of each mouse. Results are expressed as the mean ± SD (n = 6/group). (**C**) Hepatic content of lipid peroxides. Results are expressed as the mean ± SD (n = 6 /group). *P < 0.05 compared with *Ppara*$^{+/+}$ nontransgenic mice; **P < 0.05 compared with *Ppara*$^{+/-}$:HCVcpTg mice; #P < 0.05 compared with *Ppara*$^{-/-}$:HCVcpTg mice. (**D**) Immunoblot analysis of AOX, CYP4A1, catalase, and Cu, Zn-SOD. The whole-liver lysate used in the experiment in Figure 4E (20 μg protein for AOX and CYP4A1 and 50 μg for others) was loaded in each lane. The band of actin was used as the loading control. Results are representative of 4 independent experiments. **A** and **B** indicate full-length and truncated AOX, respectively. The band intensity was quantified densitometrically, normalized by that of actin, and subsequently normalized by that in *Ppara*$^{+/+}$ nontransgenic mice. The mean value of the fold changes is expressed under each band. *P < 0.05 compared with *Ppara*$^{+/+}$ nontransgenic mice.

function. The number of hepatocytes positive for 8-hydroxy-2′-deoxyguanosine (8-OHdG), an indicator of oxidative damage to nuclear DNA, was increased only in 24-month-old *Ppara*$^{+/+}$:HCVcpTg mice (Figure 5, A and B). Lipid peroxides were slightly increased in the livers of 9-month-old *Ppara*$^{+/+}$:HCVcpTg mice (data not shown) and were more abundant in the livers of 24-month-old *Ppara*$^{+/+}$:HCVcpTg mice than in those of *Ppara*$^{+/-}$:HCVcpTg and *Ppara*$^{-/-}$:HCVcpTg mice or *Ppara*$^{+/+}$ nontransgenic mice (Figure 5C). Expression of typical ROS-generating enzymes (AOX and cytochrome P450 4A1 [CYP4A1]) and ROS-eliminating enzymes (catalase and Cu, Zn-SOD) was examined. Immunoblot analysis showed marked increases in the expression of AOX and CYP4A1 and mild increases in that of catalase only in *Ppara*$^{+/+}$:HCVcpTg mice. No changes in Cu, Zn-SOD were found in the subgroups of transgenic mice (Figure 5D). These results suggest that enhanced oxidative stress causes damage in nuclear DNA and probably in mitochondria in the *Ppara*$^{+/+}$:HCVcpTg mice.

Persistent and spontaneous PPARα activation in Ppara$^{+/+}$*:HCVcpTg mice.* Liver tumorigenesis induced by long-term exposure to peroxisome proliferators and the related changes, such as sustained hepatocyte proliferation and increased oxidative stress, are associated with persistent PPARα activation (19–21). To examine the activation of PPARα, we quantified the level of PPARα mRNA, which is induced by PPARα activation (24, 25). PPARα mRNA levels were higher in 9-month-old *Ppara*$^{+/+}$:HCVcpTg mice than in *Ppara*$^{+/+}$ nontransgenic mice (Figure 6A). These increases were more pronounced at 24 months of age. However, there were no differences in PPARα mRNA levels between *Ppara*$^{+/-}$:HCVcpTg and *Ppara*$^{+/-}$ nontransgenic mice at either 9 or 24 months of age. The expression levels of typical PPARα target genes (16, 25, 26) – such as FAT, FATP, L-FABP, AOX, and MCAD (Figure 2); c-Myc, cyclin D1, CDK4, and PCNA (Figure 4); and CYP4A1 (Figure 5) – were simultaneously and synchronously increased in *Ppara*$^{+/+}$:HCVcpTg mice, but not in *Ppara*$^{+/-}$:HCVcpTg or *Ppara*$^{-/-}$:HCVcpTg mice. These results confirm that persistent activation of PPARα occurs only in *Ppara*$^{+/+}$:HCVcpTg mice. Various changes observed in *Ppara*$^{+/+}$:HCVcpTg mice, i.e., increased fatty acid uptake, mitochondrial abnormalities, steatosis, ROS overproduction, accelerated hepatocyte proliferation, and hepatocarcinogenesis, were considered to be closely linked with sustained PPARα activation.

Nuclear PPARα content. The results described above suggest that persistent PPARα activation is critical to the steatogenesis and hepatocarcinogenesis induced by the HCV core protein. A question arises as to why *Ppara*$^{+/-}$:HCVcpTg mice with an active *Ppara* allele do not exhibit the hallmarks of PPARα activation and do not develop HCC. To address this issue, the nuclear PPARα content was analyzed. Immunoblot analysis for PPARα showed that the amount of nuclear PPARα protein in *Ppara*$^{+/+}$:HCVcpTg mice was approximately 2- to 3-fold that of *Ppara*$^{+/+}$ nontransgenic mice, which was disproportionate to the higher PPARα mRNA levels (approximately 1.2- to 1.6-fold) (Figure 6, A and B). The level of nuclear PPARα in *Ppara*$^{+/-}$:HCVcpTg mice was significantly lower than that in *Ppara*$^{+/+}$:HCVcpTg mice and was similar to that in *Ppara*$^{+/+}$ nontransgenic mice (Figure 6B). Thus, the lower amount of nuclear PPARα in *Ppara*$^{+/-}$:HCVcpTg mice than in *Ppara*$^{+/+}$:HCVcpTg mice might have heightened the threshold of expression required for long-term spontaneous PPARα activation.

The degree of an increase in nuclear PPARα levels was evidently higher than the degree of an increase in PPARα mRNA levels in HCVcpTg mice (Figure 6, A and B). To investigate this disparity, the stability of nuclear PPARα was evaluated by pulse-chase experiments using isolated hepatocytes obtained from these mice. The half-life of nuclear PPARα was significantly longer (P < 0.05) in *Ppara*$^{+/+}$:HCVcpTg mice (11.5 ± 2.3 h) than in *Ppara*$^{+/+}$ nontransgenic mice (5.8 ± 1.4 h) (Figure 6C). The half-life of nuclear PPARα in *Ppara*$^{+/-}$:HCVcpTg mice tended to be prolonged compared with that in *Ppara*$^{+/-}$ nontransgenic mice (Figure 6C). These results suggest that the stability of nuclear PPARα was increased as a result of HCV core protein expression. Because it is known that the core protein interacts with retinoid X receptor α (RXRα) (27) and that

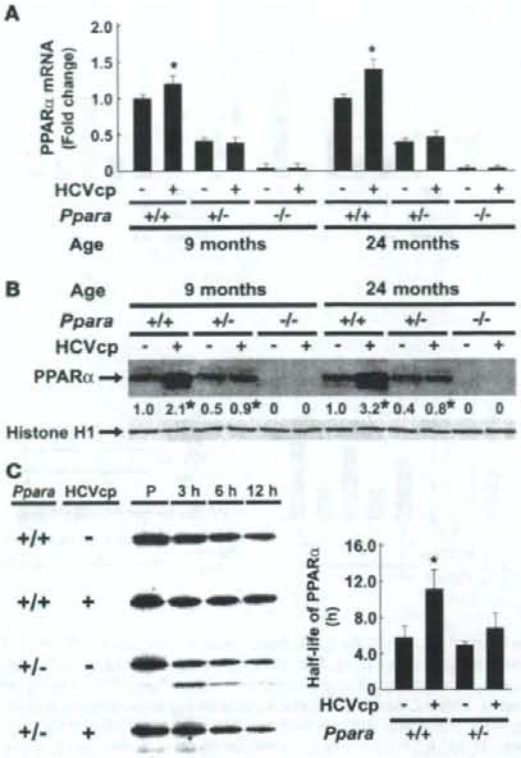

Figure 6
Persistent PPARα activation in *Ppara*$^{+/+}$:HCVcpTg mice. (**A**) PPARα mRNA levels. Total RNA was prepared from each mouse, and PPARα mRNA levels were determined by RT-PCR, normalized by those of GAPDH, and subsequently normalized by those of 9-month-old *Ppara*$^{+/+}$ nontransgenic mice. Results are expressed as the mean ± SD (n = 6 /group). (**B**) Immunoblot analysis of nuclear PPARα. The nuclear fraction obtained from each mouse (100 μg protein) was loaded in each well. The band of histone H1 was used as the loading control. Results are representative of 6 independent experiments. The band intensity was quantified densitometrically, normalized by that of histone H1, and subsequently normalized by that in 9-month-old *Ppara*$^{+/+}$ nontransgenic mice. The mean value is expressed under each band. *P < 0.05 compared with nontransgenic mice of the same age and *Ppara* genotype. (**C**) Pulse-chase experiments for 3, 6, and 12 h and pulse-label (P) experiments for nuclear PPARα using isolated mouse hepatocytes. Left: labeled PPARα bands on x-ray film. Pulse-label and pulse-chase experiments were performed as described in Methods. Results are representative of 4 independent experiments. Right: half-life of PPARα. The band intensity was measured densitometrically and subsequently normalized by that of the pulse-label experiments. The percentage of the band intensity was plotted, and the half-life of PPARα was calculated. Results obtained from 4 independent experiments are expressed as the mean ± SD. *P < 0.05 compared with nontransgenic mice in the same *Ppara* genotype.

PPARα influences the stability of RXRα (28), it is plausible that the core protein would affect its action in nuclei through an interaction with the PPARα-RXRα heterodimer and stabilization of PPARα.

Development of hepatic steatosis and HCC with long-term clofibrate treatment in Ppara$^{+/-}$*:HCVcpTg mice.* To further confirm the significance of persistent PPARα activation on core protein–induced pathological changes, *Ppara*$^{+/-}$ and *Ppara*$^{+/-}$:HCVcpTg mice were fed a standard diet containing 0.05% clofibrate for 24 months. Interestingly, hepatic steatosis appeared in the clofibrate-treated *Ppara*$^{+/-}$:HCVcpTg mice, but not in the *Ppara*$^{+/-}$ mice under the same treatment conditions (Figure 7, A and B). Similar to our observations in *Ppara*$^{+/+}$:HCVcpTg mice not treated with clofibrate, aberrant mitochondria with discontinuous outer membranes and decreased palmitic acid β-oxidation activity were found only in the clofibrate-treated *Ppara*$^{+/-}$:HCVcpTg mice (Figure 7, A and C). In addition, levels of MCAD mRNA; AOX, and CYP4A1 proteins; PPARα mRNA; and nuclear PPARα protein were higher in the clofibrate-treated *Ppara*$^{+/-}$:HCVcpTg mice than in the clofibrate-treated *Ppara*$^{+/-}$ mice (Figure 7, D–F), which suggests that the degree of PPARα activation in the former group was greater than that in the latter group and similar to that in *Ppara*$^{+/+}$:HCVcpTg mice not treated with clofibrate. Finally, the incidence of HCC after clofibrate treatment was higher in *Ppara*$^{+/-}$:HCVcpTg mice (25%; 5 in 20 mice) than in *Ppara*$^{+/-}$ mice (5%; 1 in 20 mice). Therefore, these results corroborate the importance of constant PPARα activation to the pathogenesis of hepatic steatosis and HCC in the transgenic mice.

Discussion

A novel and striking finding in this study is the absolute requirement of persistent PPARα activation for the development of HCV core protein–induced steatosis and HCC. Our data also show that the HCV core protein alone cannot induce steatosis and HCC in transgenic mice.

Mechanisms of development of steatosis in HCVcpTg mice were previously explained as an enhancement of de novo synthesis of fatty acids (29) and a decrease in MTP expression, the latter of which results in insufficient VLDL secretion from hepatocytes (30). In the present study, we revealed 2 novel mechanisms of steatogenesis in the transgenic mice, i.e., an impairment of mitochondrial β-oxidation due to the breakdown of mitochondrial outer membranes and an increase in fatty acid uptake into hepatocytes, associated with PPARα activation. PPARα activation, mitochondrial dysfunction, and hepatic steatosis appeared in 9-month-old *Ppara*$^{+/+}$:HCVcpTg mice and continued until 24 months of age, clearly preceding development of HCC. These findings thereby indicate a correlation between PPARα activation, hepatic steatosis, and HCC.

We obtained the novel and rather paradoxical finding that significant PPARα activation, which generally is expected to reduce hepatic triglyceride levels, is essential for the development of severe steatosis induced by HCV core protein. According to the results of this study, the following hypothesis concerning the development of steatosis in *Ppara*$^{+/+}$:HCVcpTg mice is proposed. First, the HCV core protein localizes partly in mitochondria (9). A recent study